Available online at www.sciencedirect.com
SCIENCE DIRECT
Journal of Solid State Chemistry 179 (2006) 1426–1433
JOURNAL OF SOLID STATE CHEMISTRY
www.elsevier.com/locate/jssc

Thermal decomposition of iron(VI) oxides, K_2FeO_4 and $BaFeO_4$, in an inert atmosphere

János Madarász[a], Radek Zbořil[b], Zoltán Homonnay[c], Virender K. Sharma[d,*], György Pokol[a]

[a]*Institute of General and Analytical Chemistry, Budapest University of Technology and Economics, Szt. Gellért tér 4, H-1521 Budapest, Hungary*
[b]*Department of Physical Chemistry, Palacky University, Svobody 26, 771 46 Olomouc, Czech Republic*
[c]*Department of Nuclear Chemistry and MTA-ELTE Research Group on the Application for Nuclear Techniques in Structural Chemistry, Eötvös Loránd University, H-1117 Budapest, Pázmány P. s. 1/A, Budapest, Hungary*
[d]*Chemistry Department, Florida Institute of Technology, 150 West University Boulevard, Melbourne, FL 32901, USA*

Received 28 November 2005; received in revised form 22 January 2006; accepted 29 January 2006
Available online 9 March 2006

Abstract

The thermal decomposition of solid samples of iron(VI) oxides, $K_2FeO_4 \cdot 0.088\ H_2O$ (**1**) and $BaFeO_4 \cdot 0.25H_2O$ (**2**) in inert atmosphere has been examined using simultaneous thermogravimetry and differential thermal analysis (TG/DTA), in combination with in situ analysis of the evolved gases by online coupled mass spectrometer (EGA–MS). The final decomposition products were characterized by ^{57}Fe Mössbauer spectroscopy. Water molecules were released first, followed by a distinct decomposition step with endothermic DTA peak of **1** and **2** at 273 and 248 °C, respectively, corresponding to the evolution of molecular oxygen as confirmed by EGA–MS. The released amounts of O_2 were determined as 0.42 and 0.52 mol pro formula of **1** and **2**, respectively. The decomposition product of K_2FeO_4 at 250 °C was determined as Fe(III) species in the form of $KFeO_2$. Formation of an amorphous mixture of superoxide, peroxide, and oxide of potassium may be other products of the thermal conversion of iron(VI) oxide **1** to account for less than expected released oxygen. The thermogravimetric and Mössbauer data suggest that barium iron perovskite with the intermediate valence state of iron (between III and IV) was the product of thermal decomposition of iron(VI) oxide **2**.

Keywords: Iron(VI) oxides; K_2FeO_4; BaFeO4; O_2 evolution; Thermogravimetry (TG); Differential thermal analysis (DTA); Evolved gas analysis (EGA); Mass spectroscopy (MS); Mössbauer spectroscopy

1. Introduction

There is an increasing interest in oxides of higher oxidation states of iron (Fe(IV), Fe(V), and Fe(VI)) because they are involved as an alternate for battery cathodes, as green oxidants for organic synthesis, as environmental-friendly oxidants in pollution remediation processes, and as intermediates in Fenton reactions and biological transfer processes [1–10]. Investigations of the synthesis conditions, stability, reactivity, and physical and chemical properties of iron compounds in higher oxidation states (over III) is of basic interest for understanding the inorganic chemistry of iron and of essential importance for various applications. Of the three higher oxidation states of iron, Fe(VI) has been proposed as a green chemical for various industrial and water treatments [11–13]. Although Fe(VI) has been known for many years, the detailed mechanism of its synthesis has not been well established.

In the laboratory, solid potassium salt of Fe(VI) oxide, K_2FeO_4, is produced by three types of synthetic techniques: wet methods, oxidizing a basic solution of a Fe^{III} salt chemically, e.g., by hypochlorite, hypobromite; electrochemically, electrolyzing a concentrated solution of NaOH and/or KOH with an iron anode, and thermally by the reaction of potassium superoxides (or potassium nitrate) with iron oxide powder heating of various solid mixtures of various substances containing potassium and iron [14–20]. The advantage of the dry method is that it does not use either sodium hydroxide or potassium hydroxide. However, the yield of the dry method is usually less than 50%. The steps involved in this synthesis method have not been

*Corresponding author. Fax: +321 674 8951.
E-mail address: vsharma@fit.edu (V.K. Sharma).

0022-4596/$ - see front matter © 2006 Elsevier Inc. All rights reserved.
doi:10.1016/j.jssc.2006.01.054

studied to learn the causes of such a low yield of ferrate(VI) product. Understanding the mechanism of the synthesis process has become essential in order to synthesize a product of solid K_2FeO_4 of high purity.

One of the possible reasons for the low yield is the simultaneous decomposition of K_2FeO_4 with increasing temperature when heating the mixture of peroxide and iron oxide to 1000 °C, a required temperature to synthesize Fe(VI). Thermal decomposition of K_2FeO_4 has been studied by many workers in 1960 and 1970s [16,21,23,24]. Scholder et al. [21,25] first studied the thermal behavior of K_2FeO_4 under oxygen stream at various times in the temperature range 200–1000 °C. The microscopic image of samples between 350 and 550 °C showed a mixture of two crystalline phases of dark and light green particles, the latter was assumed to be $KFeO_2$. The darker phase was considered as a solid solution of K_2FeO_4 and K_3FeO_4 in a 1:2 molar ratio. The overall mean oxidation number of iron species was measured to be +4.4. The overall reaction equation for the formation of pentavalent K_3FeO_4 and trivalent $KFeO_2$ as decomposition products was formulated as

$$5K_2FeO_4 = K_2FeO_4 \cdot 2K_3FeO_4 + 2KFeO_2 + 2O_2. \quad (1)$$

Later Ichida [24] also studied the thermal decomposition of K_2FeO_4 upto 1000 °C in air. An analysis of the light green residues product of the reaction indicates the formation of potassium orthoferrite(III), $KFeO_2$ with no other crystalline compound containing the potassium ion. Neither of the intermediate valence states, Fe^{5+} or Fe^{4+}, was observed during the decomposition process; in disagreement with a hypothesis reported by Scholder et al. [21]. This work formulated the chemical process shown in Eq. (2), which indicates an uncertainty in the chemical form of the potassium oxide residue:

$$K_2FeO_4 = KFeO_2 + KO_x + (2-x)/2O_2. \quad (2)$$

The barium salt of iron(VI) oxide, $BaFeO_4$, can be synthesized easily from K_2FeO_4 [25,26]. The thermal decomposition of $BaFeO_4$ was studied by Scholder et al. [16,21] and Ichida [27]. Scholder et al. [16,21] observed that $BaFeO_4 \cdot aq$ samples containing H_2O decomposed quantitatively to $BaFeO_3 \cdot aq$ on storage at room temperature. Thermal decomposition of vacuum dried $BaFeO_4 \cdot aq$ samples in the temperature range of 200–350 °C yielded a product with minimal value +3.2 of overall mean oxidation state of iron at 250 °C; suggesting incomplete decomposition to Fe(III) [16,21]. Ichida [27] found four types of $BaFeO_x$ ($2.5 < x < 3.0$) phases as thermal decomposition products of pure $BaFeO_4$ depending on temperature and O_2 pressure.

Clearly, there are literature discrepancies in the results regarding the possible formation of intermediate oxidation states of iron, Fe(V) and Fe(IV), as well as final iron oxide phases, which have not been fully characterized in the thermal decomposition of K_2FeO_4 and $BaFeO_4$. The present paper is an attempt to resolve some of the discrepancies by studying the thermal behavior and decomposition products of K_2FeO_4 and $BaFeO_4$ using simultaneous thermogravimetric and differential thermal analysis (TG/DTA) up to 500 °C in combination of in situ analysis of the evolved gases with online coupled mass spectroscopy (EGA–MS). Mössbauer spectroscopic technique was applied to find a possibe existence of intermediate iron(V) and iron(IV) oxides and to determine final product in the decomposition processes.

2. Experimental

2.1. Synthesis of K_2FeO_4 and $BaFeO_4$ samples

Iron(VI) oxide as the potassium salt (K_2FeO_4) was prepared according to the method of Thompson et al. [14]. Briefly, ferric nitrate; $Fe(NO_3)_3 \cdot 9H_2O$ was added into aqueous alkaline sodium hypochlorite solution to obtain Na_2FeO_4. Potassium hydroxide was added into the sodium ferrate(VI) solution to precipitate K_2FeO_4. The crystals of K_2FeO_4 were dried using ethanol and were stored in a vacuum desiccator. The purity of K_2FeO_4 was checked using Mössbauer spectroscopy and was found to be >98% [28]. The barium salt of iron(VI) oxide ($BaFeO_4$) was obtained by the reaction of barium chloride with a basic solution of K_2FeO_4 at 0 °C [25,26]. Rapid filtration of $BaFeO_4$(VI) gave a pure product.

2.2. Simultaneous thermogravimetry (TG) and differential thermal analysis (DTA) and online coupled in situ mass spectrometric evolved gas analysis (EGA–MS)

An STD 2960 Simultaneous DTA–TGA apparatus (TA Instruments Inc., New Castle DE, USA) was used. A heating rate of 10 °C/min, a flow rate of inert purge gas (N_2 or He) 60- 130 ml/min, sample sizes between 8 and 10 mg, high-purity α-Al_2O_3 as reference material and an open Pt crucible were employed. Mixtures of gaseous species evolved could reach a ThermoStar GDS 200 (Balzers Instruments, Brügg, Switzerland) quadruple mass spectrometer equipped with a Chaneltron detector through a heated 100% methyl deactivated fused silica capillary tubing kept at $T = 200$ °C. Data collection was carried out with QuadStar 422v60 software in multiple ion detection (MID) mode monitoring 64 channels ranging between $m/z = 15$ and 78. The measuring time was ca. 0.5 s for each channel, resulting in measuring cycles of ca. 32 s duration.

2.3. Mössbauer spectroscopy

The Mössbauer spectra were recorded at room temperature using a constant acceleration-type Mössbauer spectrometer (Ranger, USA) coupled with a PC-based multichannel analyzer (Nucleus). The spectra were stored in 512 channels. A $^{57}Co(Rh)$ source of 500 MBq activity was used, and the spectrometer was calibrated against a α-Fe foil, which is the reference of all isomer shift data given.

The spectra were evaluated with the Mosswinn 3.0i [29] code with the assumption of Lorentzian line shape.

3. Results and discussion

3.1. Thermal decomposition of $K_2FeO_4 \cdot aq$

The curves obtained in simultaneous TG–DTA of K_2FeO_4 (**1**) are shown in Fig. 1a. The oxygen evolved in thermal treatment of K_2FeO_4 (**1**) was analyzed using EGA–MS. The intensity curves of the ion fragments of O_2 evolved between 210 and 310 °C are given in Fig. 1b. Generally, two decomposition steps were observed in the TG curve up to 500 °C: one below 100 °C corresponding to evolution of water loosely adsorbed on the sample as detected also by EGA–MS, and a second step between 210 and 310 °C, when no other than O_2 gas was released from the sample (Fig. 1a and b). This observation of O_2 evolution agreed with observations made by Scholder et al. [16,21]. Both decomposition steps were accompanied by endothermic heat effects according to our simultaneous DTA measurements.

The nature of iron(III) oxide in the main decomposition step of the thermal decomposition of K_2FeO_4 sample was monitored by a Mössbauer spectroscopic technique. In this experiment, K_2FeO_4 solid sample was heated in a separate furnace at 250 °C for 1 h with protection against ambient effects. The sample (about 80 mg) was sealed between plastic foils right after removal from the furnace so that the effect of moisture could be minimized. The Mössbauer spectrum of this greenish residue is shown in Fig. 2a. The sextet observed (96.6% of the total spectrum area) represents a very characteristic signature of the $KFe^{III}O_2$ phase; its parameters (isomer shift, δ: 0.19 mm/s, magnetic field, B: 50.0 T, quadrupole splitting, Δ: 0.08 mm/s) are in agreement with those reported by Ichida [24]. This phase is metastable as shown by the Mössbauer spectrum recorded after 2 days storage at room temperature in the sealed sample holder (Fig. 2b). The spectrum of the final decomposition product in open air is shown in Fig. 2c. Newly appeared doublets indicate Fe^{III} valence states. The final isomer shift is about 0.31 mm/s, which is ~0.1 mm/s higher than that for $KFeO_2$; indicating an increase of the coordination number of iron, probably due to the chemical transformation towards iron(III) oxyhydroxide. The results of Mössbauer spectroscopy suggest that the thermal decomposition of K_2FeO_4 at 250 °C in an inert atmosphere leads directly to Fe(III) without any indications of intermediate (V) or (IV) species. The process may thus be expressed as

$$2K_2FeO_4 = 2KFeO_2 + K_2O + 3/2O_2. \quad (3)$$

Fätu and Schiopescu [23] have suggested Eq. (4) to account for the formation of oxygen. Eqs. (3) and (4) are similar in terms of moles of oxygen formed from the decomposition of K_2FeO_4, however, the Fe_2O_3 unit suggested in Eq. (4) contradicts the Mössbauer data:

$$2K_2FeO_4 = K_2O \cdot Fe_2O_3 + K_2O + 3/2O_2 \quad (4)$$

The thermo-analytical investigations of a K_2FeO_4 sample in work of Fätu and Schiopescu [23] gave a loss of 14.28% of the initial mass. This loss was fully assigned to the release of 3/4 O_2 for each mole of decomposed K_2FeO_4, according to Eq. (4). However, the calculated theoretical mass from Eq. (4) is 12.12%, which is smaller than the observed value. No explanation was provided for

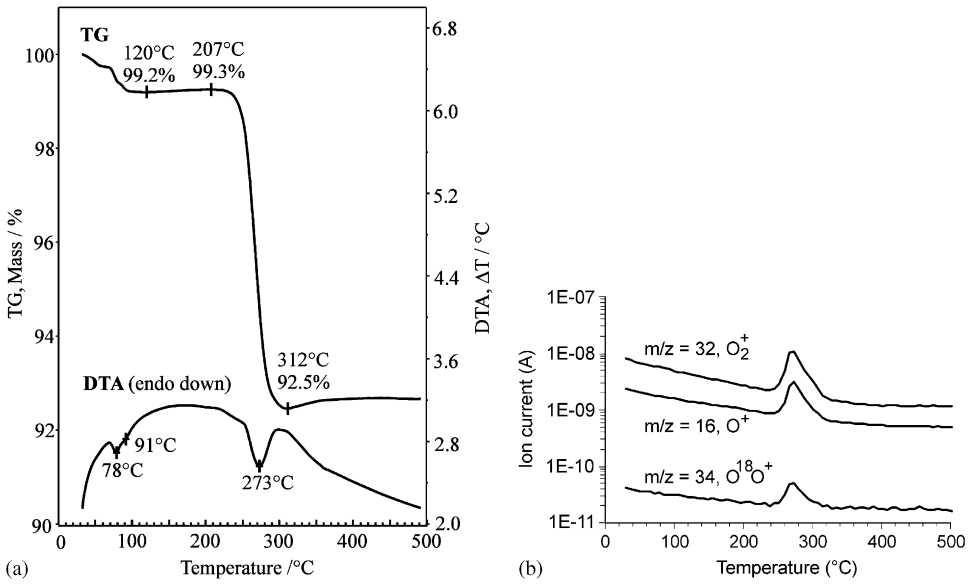

Fig. 1. (a) Simultaneous TG/DTA curves (mass changes and heat effects) of sample K_2FeO_4 (initial mass 8.93 mg, 130 ml/min N_2, 10 °C/min). (b) Intensity courses of ion fragments of O_2 evolved from sample K_2FeO_4 (**1**) measured in pure He by an online coupled TG/DTA–MS system (initial mass 9.94 mg, 60 ml/min He, 10 °C/min).

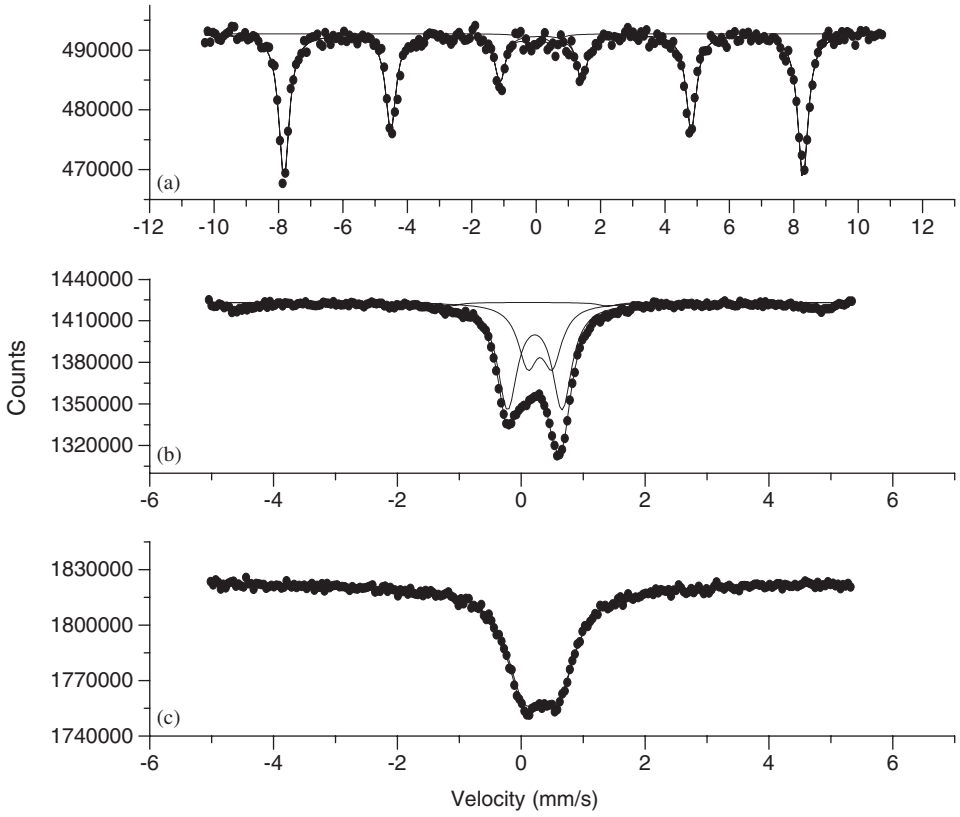

Fig. 2. Room temperature Mössbauer spectrum of the decomposition product $KFeO_2$ obtained after heat treatment of K_2FeO_4 at 250 °C (a), spectrum recorded after 2 days storage at room temperature in the sealed sample holder (b), and the spectrum of the final decomposition product in open air (c) indicating further decomposition. (Please note the different velocity scale.)

the 2% excess weight loss. More recently, Tsapin et al. [30] also studied the thermal decomposition of K_2FeO_4. The two main steps in the TG curve in this study gave an overall 16.18% weight loss, which is again higher than the expected value obtained from Eq. (4). If one considers the first step with 7.214% mass loss (up to $T = 125\,^{\circ}C$) as amount of desorbed water, then 8.76% of the original sample can be considered as the amount of the evolved oxygen. Though this latter value is close to the observation made by Scholder et al. [21], it is much lower than the expected value (12.12%).

Our experiments in the TG/DTA–MS measuring system confirmed that only 0.8% bound water molecules were evolved up to 120 °C in the first step, which was followed by oxygen (O_2) release between 210 and 310 °C. The amount of oxygen was 6.8% of the original weight. In comparison, our samples contained much less water than the samples of Tsapin et al. [30]. The extent of oxygen gas evolution observed in our work was only ca. 56% of the expected theoretical value (12.12%, Eq. (3)), which is similar to the values obtained by Tsapin et al. [30] and Scholder et al. [16]. It is reasonable to assume that not all the oxygen was released during the conversion of Fe(VI) to Fe(III) in the main decomposition step (around 270 °C). The final product of the decomposition probably contains a noncrystalline mixture of potassium superoxide, potassium peroxide, and potassium oxide. Oxygen being retained in form of peroxide and/or superoxide itself may explain the lower than expected weight loss.

3.2. Thermal decomposition of $BaFeO_4 \cdot aq$

The TG/DTA curves of $BaFeO_4 \cdot aq$ (**2**) are shown in Fig. 3a. The TG curve shows a water loss below and above 100 °C; indicating the presence of weakly as well as strongly bound water molecules in the sample. The intensity curves of the ion fragments of O_2 evolved from the $BaFeO_4 \cdot aq$ (**2**) sample between 190 and 270 °C are given in Fig. 3b. Similar to the decomposition of K_2FeO_4 (**1**), $BaFeO_4 \cdot aq$ (**2**) gave two decomposition steps in TG up to 400 °C. The first decomposition step between 120 and 180 °C corresponds to water evolution and a little O_2 release, detected by EGA–MS. A second step between 190 and 270 °C released only O_2 from the sample (Fig. 3). This latter observation on O_2 evolution is consistent with the results of Scholder et al. [16,21]. DTA measurement indicates that both decomposition steps were accompanied by endothermic heat effects.

The results of the TG/DTA–MS system were used to determine the percentage of released water. In the first step,

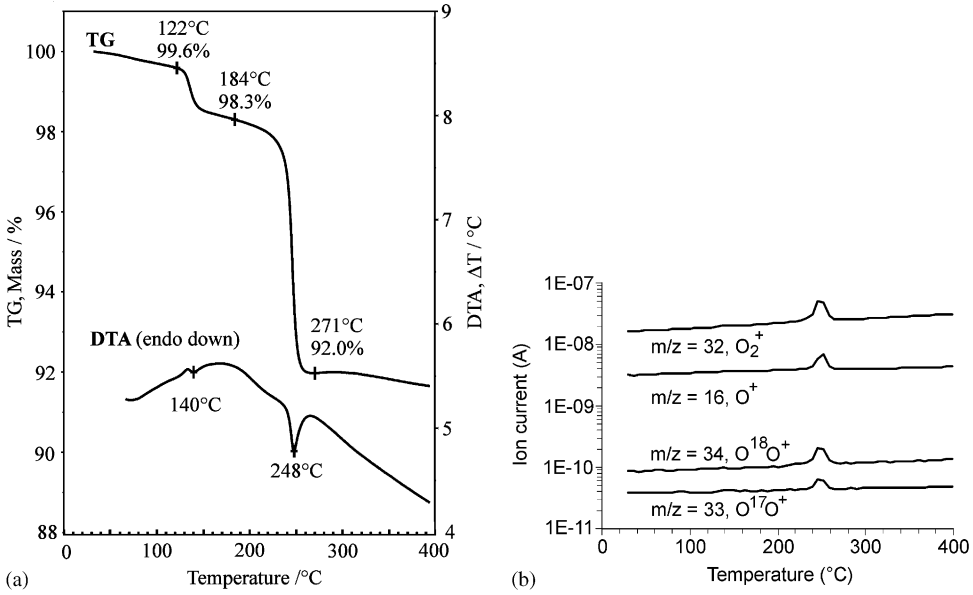

Fig. 3. (a) Simultaneous TG/DTA curves (mass changes and heat effects) of $BaFeO_4 \cdot aq$ (**2**) sample (initial mass 10.08 mg, 130 ml/min N_2, 10 °C/min). (b) Intensity courses of ion fragments of O_2 evolved from sample $BaFeO_4 \cdot aq$ (**2**) measured in pure N_2 by online coupled in situ TG/DTA–MS system (initial mass 10.08 mg, 130 ml/min N_2, 10 °C/min).

0.4% of loosely bond water was released till 120 °C, followed by evolution of 1.3% strongly bound water molecules in the temperature range 120–170 °C. The release of oxygen gas occurred between 180 and 270 °C, the amount of which was 6.3% of the original weight. Our results are little different from the recent measurement made by Ni et al. [31] and Yang et al. [32] on the specially prepared $BaFeO_4$ samples. Ni et al. [31] used special drying methods to prepare the $BaFeO_4$ sample, which gave a loss of 0.9% adsorbed water up to 250 °C with a release of 4.8% oxygen at 260 °C. The amount of evolved oxygen corresponds to ca. 0.77 mol oxygen atom per formula unit of anhydrous $BaFeO_4$, which is only one half of the expected 0.75 moles of molecular oxygen released around 260 °C [31]. Yang et al. [32] observed 0.99% weight loss at about 131 °C of vacuum dried $BaFeO_4$ samples. This was attributed to the loss of adsorbed water. The initial water and carbonate content in $BaFeO_4$ samples have shown effects on the TG curves and the decomposition schemes up to 250 °C [31,32].

In the vacuum dried sample, a 6.36% weight loss of the original weight was observed at ~255 °C, which corresponds to ca. 1 mol oxygen atom per formula unit of $BaFeO_4 \cdot aq$ (**2**) [32]. The amount of water in $BaFeO_4$ samples may have caused discrepancies in the observed results. The samples in our work contained more water (~0.25 mol H_2O per formula unit) than the samples of Ni et al. [31] and Yang et al. [32]. This difference in water content results in almost the same amount of oxygen gas evolution (1.03 mol oxygen atom per formula unit) compared to data of Yang et al. [32], while the amount of released oxygen is higher than that observed by Ni et al. [31]. The O_2 released in the main decomposition step (around 250 °C) of the thermal decomposition of $BaFeO_4 \cdot aq$ samples might be even more than 0.5 mol O_2 pro formula unit because of the possible formation of $BaFeO_x$ ($2.5 < x < 3.0$) phases. Ichida [26] observed the formation of the tetragonal phase with composition $BaFeO_{2.61-2.71}$. This tetragonal phase was stable below 400 °C.

It is well known, however, that perovskites of ABO_3 structure with Fe at site B and alkaline earths at site A have a tendency to form rather stable Fe^{IV} compounds. Most stable perovskites were found to be $SrFeO_{3-d}$ with d very close to zero when synthesized in presence of oxygen under pressure. $BaFeO_{3-d}$ can also be prepared, however, its Mossbauer spectrum contains an asymmetrical doublet, the analysis of which is difficult. Gallagher et al. [33], who prepared hexagonal $BaFeO_{3-d}$ by solid-state synthesis suggested that the Mossbauer spectrum may be formally evaluated as a superposition of two singlets; one representing Fe^{III} while the other one representing a valence state in between Fe^{III} and Fe^{IV}. In the hexagonal lattice, there are two nonequivalent octahedral Fe sites with significant number of vacancies.

Room temperature Mössbauer spectra of a partially decomposed and a fully decomposed $BaFeO_4$ sample at room temperature under inert atmosphere are shown in Fig. 4a and 4b, respectively. Hyperfine parameters of both spectra are summarized in Table 1. The larger component with isomer shift $\delta = 0.34$–0.37 mm/s can be assigned to a regular octahedrally coordinated Fe^{III} site. The smaller component ($\delta = -0.01$–0.07 mm/s) may be due to an O-defect associated Fe-site having the intermediate valence state (between III and IV). It is therefore difficult to calculate oxygen stoichiometry of

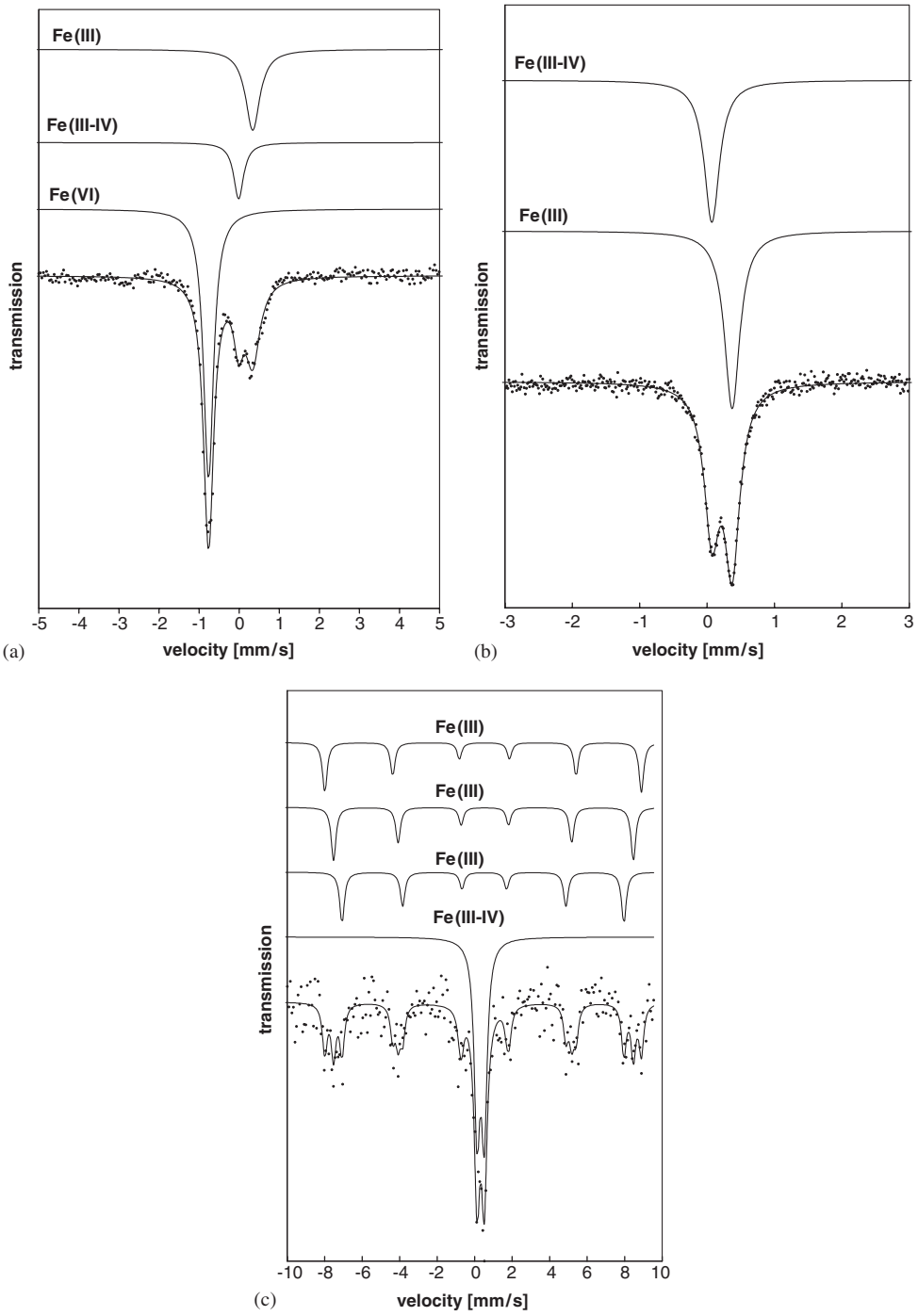

Fig. 4. Room temperature Mössbauer spectra of the decomposition product $BaFeO_{3-d}$ obtained after heat treatment of $BaFeO_4$ at 250 °C for 5 min (a), not fully decomposed sample and at 300 °C for 1 h (b) and spectrum of a fully decomposed sample recorded at 5 K (c).

the compound on basis of the Mössbauer parameters and relative abundances of the singlets.

To further evaluate the structure of the $BaFeO_{3-\delta}$ phase more precisely and to confirm the correctness of the mathematical processing of the room temperature spectra, low temperature (5 K) Mössbauer measurements of a fully decomposed $BaFeO_4$ sample were performed (see Fig. 4c and Table 1). There are four spectral components, three sextets and one doublet. Magnetically ordered components with isomer shift $\delta = 0.48$–0.50 mm/s and hyperfine magnetic fields $H_{hyp} = 46.7$; 49.7 and 52.4 T correspond to high-spin iron(III) in different octahedral environments. The number of iron atoms in various octahedral positions seems to be equivalent as reflected through almost the same spectral areas (18.6–19.3%). The paramagnetic component with lower isomer shift $\delta = 0.30$ mm/s could be assigned to iron in a valence state in between Fe^{III} and Fe^{IV}, in accordance with the spectral area (43%) being close to that

Table 1
Mössbauer parameters of decomposition products of $BaFeO_4$ (A-sample heated at 250 °C, 5 min; B-sample heated at 300 °C, 1 h)

Sample	T [K]	Component	δ [mm/s]	$\varepsilon_Q(\Delta E_Q)$ [mm/s]	H_{hyp} [T]	RA [%]	Assignment
	300	Singlet	−0.76	—	—	65	Fe(VI)
A		Singlet	−0.01	—	—	15.5	Fe(III–IV)
		Singlet	0.34	—	—	19.5	Fe(III)
B	300	Singlet	0.07	—	—	44.0	Fe(III–IV)
		Singlet	0.37	—	—	56.0	Fe(III)
B	5	Doublet	0.32	0.38	—	43.0	Fe(III–IV)
		Sextet	0.48	−0.07	46.7	19.1	Fe(III)
		Sextet	0.50	−0.07	49.7	19.3	Fe(III)
		Sextet	0.48	−0.07	52.4	18.6	Fe(III)

T—temperature of measurement, δ—isomer shift related to metallic iron, $\varepsilon_Q(\Delta E_Q)$—quadrupole shift (quadrupole splitting), H_{hyp}—hyperfine magnetic field, RA—relative spectrum area.

of $Fe^{III–IV}$ in the room temperature spectrum (44%). Nevertheless, its isomer shift at 5 K is higher than expected solely due to the temperature lowering (“temperature shift”). It seems to be that the itinerant electrons become partially localized upon cooling and higher electron density was observed on the Fe3*d* levels [34]. The results thus clearly provide indirect evidence of the formation of a nonstoichiometric $BaFeO_{3-\delta}$ phase with some amount of Fe ions in the intermediate valence state (III–IV) being paramagnetic at 5 K.

Our Mössbauer observations of final product of the thermal decomposition of $BaFeO_4$ are in disagreement with the previous results of Gallagher’s [33] and Ichida’s [27] made at room temperature. The Mossbauer spectra in these studies have an opposite intensity asymmetry in comparison with our results. This indicates that the relative fraction of the Fe^{III} species (centered at higher velocities) to $Fe^{III,IV}$ species (at lower velocities) is higher in our study than that of earlier studies. The higher Fe^{III} content means more ionicity, causing more localized electrons. The difference between the samples is most probably the oxygen stoichiometry, which is critical in determining the electronic structure. The decomposition of $BaFeO_4$ obviously did not result in stoichiometric “$BaFe^{IV}O_3$” although oxygen is abundantly available for Fe during the decomposition. Surprisingly, our product apparently has lower average valence state for Fe than Gallagher’s compound prepared from the Fe^{III} oxidation state compound. This indicates the importance of the history of a particular sample. Products of $BaFeO_4$ are also influenced by aging of the solid sample. This was recently demonstrated in two studies on disintegration of barium and potassium ferrates(VI) due to the sample aging [35] and long-term low-temperature (45 °C) heating [36]. Both studies though showed $BaFeO_4$ transformation to iron(IV) species, $BaFeO_3$, in a primary decomposition step, but final product of the secondary step differs. Nowik et al. [35] suggested the mixture of BaO and Fe_2O_3 nanoparticles, while Ayers and White [36] proposed the formation of $BaFeO_{2.5}$. Interestingly, in contrast to barium ferrate(VI), the decomposition process of potassium ferrate(VI) results in the direct formation of Fe(III) species; no stable Fe(IV) or Fe(V) intermediates were detected in aged samples.

4. Conclusions

The TG/DTA–EGA–MS and Mössbauer measurements of $K_2FeO_4 \cdot 0.08H_2O$ and $BaFeO4 \cdot 0.25H_2O$ samples established the percentage of adsorbed and/or bound water molecules, the amount of oxygen released, and the form of iron(III) in the decomposing product. The results did not provide any evidence of the formation of intermediate oxidation states, iron(V) and iron(IV) in the case of the potassium salt, while partial Fe(IV) formation was found for the barium salt. The temperature range of the main degradation step of the iron(VI) oxides when molecular O_2 is released and Fe(III) species are formed was 170–320 °C, which was almost independent of the nature of the cation in the iron(VI) oxide. This indicates that the stability of iron(VI) oxides are basically determined by the $Fe^{VI}O_4^{2-}$ anion. The thermal synthesis of iron(VI) oxides occurs at 700–900 °C [15], which is well above the stability range. This may be the cause of the low yield in the thermal synthetic process even with the use of a large excess of oxidants. A considerable amount of oxygen is found to be partially retained, which may be explained by the formation of an amorphous mixture consisting of superoxide and peroxide of potassium in the case of K_2FeO_4 and by the formation of ferrate(III,IV) in the case of $BaFeO_4$. Such a highly reactive residual product in the sample of iron(VI) oxide may not be useful for applications in super-ion batteries. However, these residual products will provide additional oxidation power in treating pollutants in wastewater.

Acknowledgments

We appreciate the support gained from the NATO Collaborative Linkage Grant (EST.CLG No. 979931) and from the Projects of Ministry of Education of the Czech Republic (1M6198959201 and MSM6198959218).

References

[1] L. Delaude, P. Laszlo, J. Org. Chem. 61 (1996) 6360–6370.
[2] S. Licht, B.H. Wang, S. Ghosh, Science 285 (1999) 1039–1042.
[3] V.K. Sharma, Adv. Environ. Res. 6 (2002) 143–156.
[4] J. Jiang, B. Lloyd, Water Res. 36 (2002) 1397–1408.
[5] V.K. Sharma, F. Kazama, H. Jiangyong, A.K. Ray, J. Water Health 3 (2005) 45–58.
[6] E.Y. Tshuva, S.J. Lippard, Chem. Rev. 104 (2004) 987.
[7] M. Coasts, M.P. Mehn, M.P. Jensen, L. Que Jr., Chem. Rev. 104 (2004) 939–986.
[8] O. Pestovsky, A. Bakac, J. Am. Chem. Soc. 126 (2004) 13757–13764.
[9] A. Ghosh, F.T. de Oliveira, T. Yano, T. Nishioka, E.S. Beach, I. Kinoshita, E. Munck, A.D. Ryabov, C.P. Horwitz, T.J. Collins, J. Am. Chem. Soc. 127 (2005) 2505–2513.
[10] L. Deguillaume, M. Leriche, K. Desboeufs, G. Mailhot, C. George, N. Chaumerliac, Chem. Rev. 105 (2005) 3388–3431.
[11] V.K. Sharma, Water Sci. Technol. 49 (2004) 69–74.
[12] V.K. Sharma, C.R. Burnett, R. Yngard, D. Cabelli, Environ. Sci. Technol. 36 (2005) 4182–4186.
[13] S. Licht, R. Tel-Vered, R. Chem. Commun. (2004) 628–629.
[14] G.W. Thompson, G.W. Ockerman, J.M. Schreyer, J. Am. Chem. Soc. 73 (1951) 1279–1281.
[15] Y.D. Perfiliev, V.K. Sharma, in: V.K. Sharma, J.Q. Jiang, K. Bouzek (Eds.), Innovative Ferrate(VI) Technology in Water and Wastewater Treatment, 2004, pp. 32–37.
[16] R. Scholder, H. Bunsen, F. Kindervater, W. Zeiss, Z. Anorg. Allgem. Chem. 282 (1955) 268–279.
[17] F. Lapicque, G. Valentin, Electrochem. Commun. 4 (2002) 764–766.
[18] S. Licht, R. Tel-Vered, L. Halperin, J. Electrochem. Soc. 151 (2004) A31–A39.
[19] K. Bouzek, Coll. Czech. Chem. Commun. 65 (2002) 133–140.
[20] Y.M. Kiselev, N.S. Kopelev, N.A. Zavyalova, Y.D. Perfilev, P.E. Kazin, Russ. J. Inorg. Chem. 34 (1989) 1250–1253.
[21] R. Scholder, Anges. Chem. 1 (1962) 220–224.
[23] D. Fätu, A. Schiopescu, Rev. Roum. Chim. 19 (1974) 1297–1302.
[24] T. Ichida, Bull. Chem. Soc. Japan 46 (1973) 79–82.
[25] J.R. Gump, W.F. Wagner, J.M. Schreyer, Anal. Chem. 26 (1954) 1957.
[26] J.M. Schreyer, J.W. Thompson, L.T. Ockerman, Anal. Chem. 22 (1950) 691–692.
[27] T. Ichida, J. Solid State Chem. 7 (1973) 308–315.
[28] N.S. Kopelev, in: A. Vértes, Z. Homonnay (Eds.), Mössbauer Spectroscopy of Sophisticated Oxides, Akadémiai Kiadó, Budapest, 1997, pp. 305–333.
[29] Z. Klencsár, E. Kuzmann, A. Vértes, J. Rad. Nucl. Chem. 210 (1996) 105–118.
[30] A.I. Tsapin, M.G. Goldfeld, G.D. McDonald, K.H. Nealson, B. Moskovitz, P. Solheid, K.M. Kemner, S.D. Kelly, K.A. Orlandini, Icarus 147 (2000) 68–78.
[31] X.-M. Ni, M.-R. Ji, Z.-P. Yang, H.-G. Zheng, J. Cryst. Growth 261 (2004) 82–86.
[32] W. Yang, J. Wang, T. Pan, F. Cao, J. Zhang, C. Cao, Electrochim. Acta 49 (2004) 3455–3461.
[33] P.K. Gallagher, J.B. MacChesney, D.N.E. Buchanan, J. Chem. Phys. 43 (1965) 516–519.
[34] R. Zboril, M. Mashlan, D. Petridis, Chem. Mater. 14 (2002) 969–982.
[35] I. Nowik, R.H. Herber, M. Koltypin, D. Aurbach, S. Licht, J. Phys. Chem. Solids 66 (2005) 1307–1313.
[36] K.E. Ayers, N.C. White, J. Electrochem. Soc. 152 (2005) A467–A473.

Further reading

[22] A. Ito, K. Ono, J. Phys. Soc. Japan 26 (1969) 1548.